Local order and dynamic properties in liquid Au-Ge eutectic alloys by *ab initio* molecular dynamics

A. Pasturel[1,2] and N. Jakse[1,*]

[1]*Sciences et Ingénierie des Matériaux et Procédés, INP Grenoble, UJF-CNRS 1130, rue de la Piscine, BP 75, 38402 Saint-Martin d'Hères Cedex, France*

[2]*Laboratoire de Physique et Modélisation des Milieux Condensés, Maison des Magistères, BP 166 CNRS, 38042 Grenoble Cedex 09, France*

(Received 26 June 2011; published 5 October 2011)

We report the results of first-principles molecular dynamics simulations for liquid and undercooled eutectic $Au_{72}Ge_{28}$ alloys at various temperatures. In comparison with the parent $Au_{81}Si_{19}$ liquid, we find a much less pronounced chemical short-range order in $Au_{72}Ge_{28}$, mainly due to the increasing influence of Ge-Ge nearest neighbor packing. In addition, a structural analysis using three-dimensional pair-analysis techniques evidences an icosahedral short-range order and its evolution with temperature, closer to that of pure Au than to that of $Au_{81}Si_{19}$. We use such differences to understand the dynamic properties of both systems and to discuss disparities in other properties of $Au_{72}Ge_{28}$ and $Au_{81}Si_{19}$ alloys.

DOI: 10.1103/PhysRevB.84.134201 PACS number(s): 61.25.Mv, 61.20.Ja, 66.10.−x

I. INTRODUCTION

The phenomenon of undercooling in metallic systems—that is, the preservation of a metastable liquid state well below the melting point[1] —has led to speculation that local atomic structures characterized by dense but nonperiodic packing act as the main barrier for crystal nucleation.[2] These local structures, models of icosahedral short-range order (ISRO) are now widely accepted as the origin of undercooling effects since the experimental evidence of their existence has been supplied[3–5] and *ab initio* molecular dynamics (AIMD) also reveal the presence of atoms arranged with the fivefold symmetry in significant proportion.[6]

Among them, metal-semiconductor alloys like Au-Si and Au-Ge systems have drawn considerable attention in particular due to the presence of a deep eutectic region where the melting point decreases to 363 °C for $Au_{81}Si_{19}$ (Ref. 7) and 361 °C for $Au_{72}Ge_{28}$ (Ref. 7), as compared with melting temperatures of 1064, 1414, and 938 °C for pure Au, Si, and Ge, respectively. From a fundamental point of view, the reasons for their unusually deep eutectic points are not fully understood, and in the bulk, they present only a negligible tendency to undercooling. Such systems are also important for technological applications since Au-Si and Au-Ge eutectic alloys are used as a catalyst for manufacturing Si and Ge nanowires, via a vapor-liquid-solid or vapor-solid-solid mechanisms. In such applications, Schülli *et al.*[8] have recently shown that a substrate can enhance undercooling in Au-Si eutectic droplets.

Very recently, we reported first-principles molecular dynamics simulations for liquid and undercooled eutectic $Au_{81}Si_{19}$ alloys at various temperatures.[9] We showed that the local structure of this eutectic alloy is characterized by a well-defined chemical short-range order (CSRO) that enhances Au-Si interactions in contrast with the solid mixture and may explain the high stability of the liquid phase on the basis of preferential Au-Si bonds. We also demonstrated that the other consequence of the Si-alloying effect is to lower the icosahedral ordering and then to boost the atomic mobility with self-diffusion coefficients characteristic of the liquid state down to the eutectic temperature. This makes relevant the question whether a similar behavior exists in the eutectic $Au_{72}Ge_{28}$ alloy. In many aspects, Au-Ge resembles Au-Si since both systems display deep eutectics, and there are no known stable intermetallic compounds. However, recent experimental studies have shown important differences in both eutectic phases. Whereas liquid eutectic $Au_{81}Si_{19}$ exhibits a strong layering normal to the surface that is accompanied by an in-plane 2D crystalline long-range order,[10] the liquid $Au_{72}Ge_{28}$ only shows a modest, standardlike surface layering.[11] The coordinations in the eutectics also show disparities.[12] Such a difference can be related to the kind of short-range order occurring in the bulk liquid phases, i.e. to the chemical interactions between Au and Si and on the other hand between Au and Ge. Very recently, first-principles electronic calculations predict the existence of crystalline compounds around the eutectic compositions of both systems[13,14] but with different crystallographic structures, confirming that Au-Si and Au-Ge interactions are only superficially similar.

In order to address further the important question of the local structure in liquid eutectic $Au_{72}Ge_{28}$, we have performed a series of full *ab initio* molecular dynamics simulations within the density functional theory (DFT) for the stable and undercooled states. A deeper understanding of the differences with the parent Au-Si system is gained by comparing results to those obtained for the pure liquid Au and liquid Au-Si eutectic alloy[9] and examining the evolution of the local ordering as a function of the temperature. For the eutectic alloy, our findings show that the local structure is characterized by a weak Au-Ge affinity, leading to a chemical short-range order much less pronounced than in $Au_{81}Si_{19}$. Another deviation is a larger icosahedral short-range order and an evolution with temperature closer to that of pure Au than that of $Au_{81}Si_{19}$. Such dissimilarities in the short-range order are used to understand the dynamic properties of both systems and to discuss the observed differences in other properties of $Au_{72}Ge_{28}$ and $Au_{81}Si_{19}$ alloys.

II. COMPUTATIONAL BACKGROUND

The AIMD simulations were carried out using the DFT as implemented in the Vienna *ab initio* simulation package.[15] Projected augmented plane waves[16] (PAWs) with the Perdew–Wang exchange-correlation potentials have been adopted. The

valence state of each element was defined previously in the provided PAW potentials and the plane-wave cutoff is 245 eV. No relativistic effects on Au atoms were taken into account. We carried out all the dynamical simulations in the canonical ensemble (NVT) by means of a Nosé thermostat to control temperature. Newton's equations of motion were integrated using the Verlet algorithm in the velocity form with a time step of 3 fs. We have considered a system of 256 atoms in a cubic box with periodic conditions. We consider only the Γ-point to sample the supercell Brillouin zone. For $Au_{72}Ge_{28}$ alloy, the initial configuration was taken from the well-equilibrated liquid $Au_{81}Si_{19}$ system in which some Au and Si atoms were randomly substituted with Ge atoms. The volume of the cell was fixed to reproduce the experimental densities.[9,17] The resulting pressures were always positive, both for $Au_{72}Ge_{28}$ and $Au_{81}Si_{19}$ alloys, but did not exceed 0.5 GPa whatever the temperature. First, the system is equilibrated at $T = 1400$ K for 3 ps; the run was continued for 60 ps. Then the system is quenched successively to $T = 1200$, 1000, 800, and 700 K, mentioning that the same equilibration protocol at 1400 K was used for each temperature. The procedure is repeated in the undercooled region for $T = 600$ and 500 K, taking advantage of the large cooling rate provided by AIMD simulations, 5×10^{12} Ks^{-1}, to explore the metastable undercooled state. In these cases, the lengths of the runs were extended to 200 ps. For each temperature, 2000 configurations were used to produce averaged structural quantities, such as the partial pair-correlation functions. Among these configurations, 10 were selected at regularly spaced time intervals to extract their inherent structures.[18]

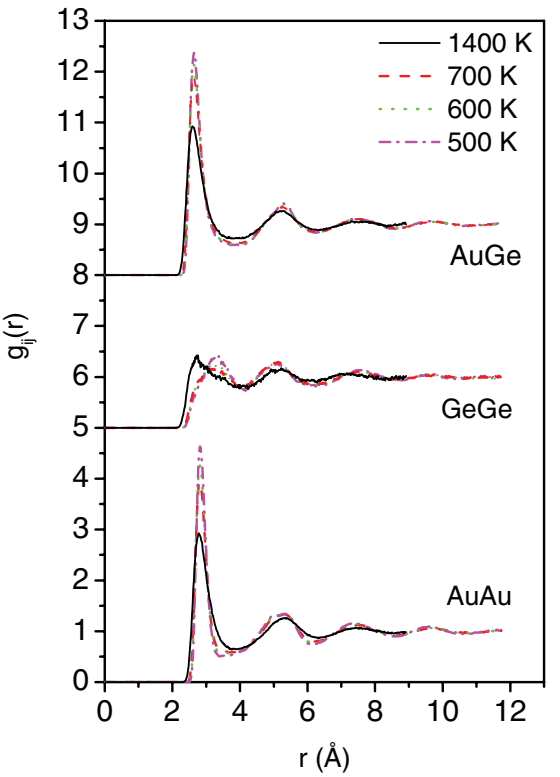

FIG. 2. (Color online) Partial pair-correlation functions of $Au_{72}Ge_{28}$ as a function of temperature. The curves for Ge-Ge and Au-Ge partials are shifted by an amount of 5 and 7, respectively.

III. RESULTS AND DISCUSSION

A. Structural properties

Figure 1 illustrates the total structure factor $S(q)$ calculated at $T = 700$ K and its comparison with the experimental one measured at $T = 666$ K by using neutron diffraction.[17] Note that we obtain a good agreement between the two sets of data, as it was already the case for the parent $Au_{81}Si_{19}$ alloy.[17] The simulated $S(q)$ does not display a clear prepeak as seen in the experimental data but only a small shoulder around 1.8 Å. This feature could be a signature of a medium-range order (MRO), as was already suggested.[19] However, due to the small size of simulation box, we will refrain from drawing conclusions on the MRO scale.

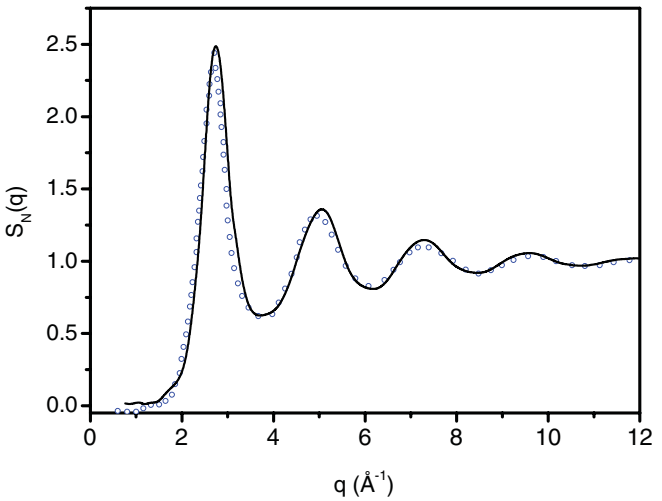

FIG. 1. (Color online) The total structure factor $S(q)$ calculated at $T = 700$ K (solid line) and compared to the experimental one (Ref. 17) measured at $T = 666$ K (open circles).

In order to examine the evolution of SRO in $Au_{72}Ge_{28}$, we have calculated several structural quantities in order to emphasize their evolution as a function of temperature. We have considered the partial pair-correlation functions $g_{ij}(r)$, as shown in Fig. 2 for liquid and undercooled states. They are important quantities to characterize local structures of liquid alloys since $g_{ij}(r)$ is defined to be the number of atoms j found at distance r from an atom i. We have determined the nearest neighbor coordination number z^1_{AuAu}, z^1_{AuGe}, and z^1_{GeGe} by counting the number of atoms in the first coordination shells directly from the configurations, which is equivalent to integrating the radial distribution functions $\mathrm{RDF}_{ij}(r)$ $c_j 4\pi\rho r^2 g_{ij}(r)$ (ρ being the atomic density) up to the first minimum of $g_{ij}(r)$. Their evolutions as a function of temperature are shown in Fig. 3.

As a first step, we discuss the evolution of the partial pair-correlation functions as a function of temperature. Upon undercooling, the evolution is mainly characterized by the increase of the first peaks of Au-Au and Au-Ge partials and a better resolution of the first peak of the Ge-Ge partial. Another important feature is the relative height of the first peaks of Au-Ge and Ge-Ge partials. It is a clear indication that the liquid phase is characterized by an intermixing between Au

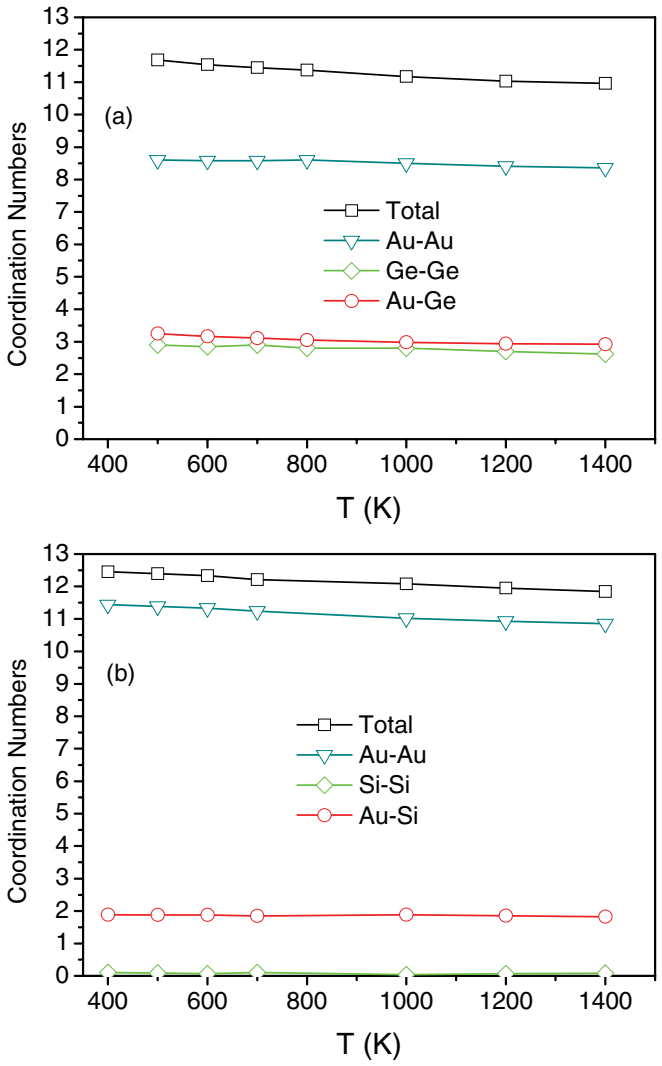

FIG. 3. (Color online) Evolution of the nearest neighbor coordination numbers, z^1_{Total}, z^1_{AuAu}, z^1_{AuGe}, and z^1_{GeGe} for Au, (a) $Au_{72}Ge_{28}$, and (b) $Au_{81}Si_{19}$ as a function of temperature.

and Ge atoms, and this behavior contrasts with the known thermodynamically stable solid made of two separate phases. However, the Ge-Ge contacts become important, in contrast to the Si-Si contacts in $Au_{81}Si_{19}$. At 700 K, just above the eutectic temperature, the partial coordination of the Ge atoms surrounding a Ge central atom is around 2.90, while for Si-Si it is found to be less than 0.1 (Ref. 9). Moreover, the total coordination number of an Au atom as well as the total coordination number in $Au_{72}Ge_{28}$ is smaller than those obtained in $Au_{81}Si_{19}$, as shown in Fig. 3. These findings indicate that $Au_{72}Ge_{28}$ displays a more open packing mainly due to the increase of the concentration of Ge atoms. They also corroborate the model of Waghorne *et al.*,[20] who proposed the existence of close packing in the liquid phases of the Au-(Si,Ge) alloys in the composition range 0–20/25 at% of the (Si,Ge) element and a more open packing for higher compositions in (Si,Ge).

To obtain a more quantitative estimate for the CSRO and its dependence with temperature, we consider the Warren CSRO parameter α_1 generalized by Wagner and Ruppersberg[21] to systems with size effects. Here, α_1, and its normalized value α_1^0 with respect to the maximum order parameter $\alpha_1^{\max}$, are calculated as follows:

$$\alpha_1 = 1 - z^1_{ij}/c_j\left(c_i z^1_j + c_j z^1_i\right), \tag{1}$$

with $z^1_i = z^1_{ii} + z^1_{ij}$ $(i, j = \text{Ge, Au})$

$$\alpha_1^0 = \alpha_1/\alpha_1^{\max} \quad \text{and} \quad \alpha_1^{\max} = 1 - z^1_i/c_j\left(c_i z^1_j + c_j z^1_i\right), \tag{2}$$

where c_j is the concentration of j species. The calculated values of α_1^0 for the liquid and undercooled states of $Au_{72}Ge_{28}$ displays only nonzero values in the undercooled regime, namely 0.028 and 0.043 at $T = 600$ and 500 K, respectively. Such values indicate that CSRO is very small in $Au_{72}Ge_{28}$, the distribution of Ge atoms around Au atoms being close to a random distribution. On the contrary, the high values α_1^0 obtained for $Au_{81}Si_{19}$, namely 0.90 and independent of the temperature, confirm that the CSRO is important in its liquid and undercooled states.[9] Thus, our results obtained for $Au_{72}Ge_{28}$ do not support the idea that the stability of the eutectic liquid is related only to the maximization of Au-Ge interaction, as it is the case for $Au_{81}Si_{19}$ (Ref. 22).

More insight into the structural changes is gained by analyzing the inherent structures and using the common-neighbor analysis (CNA)[23] that is able to give a detailed three-dimensional image of the topology surrounding each atom. Technically, the first two peaks of the pair-correlation function are decomposed, and the CNA is able to characterize the local environment surrounding each atomic pair that contributes to the peaks of $g(r)$, in terms of the number and properties of common nearest neighbors of the pair under consideration. Each bonded pair of atoms is classified according to the number and topology of the common neighbors using a set of four indices. (i) The first index denotes to what peak of $g(r)$ the pair under consideration belongs, i.e. the root pair—1 for the first and 2 for second peak of $g(r)$. (ii) The second index represents the number of nearest neighbors that bond with both of root pairs. (iii) The third index is for the number of the bonds that connect the shared nearest neighbor atoms. (iv) A fourth index is used to distinguish configurations with the same first three indices but with a different topology. The CNA can distinguish between the fcc, hcp, bcc, and icosahedral packing as well as more complex polytetrahedral environments (see Ref. 10 for more details).

We considered bonded pairs for which the root pair has at least one Au atom in $Au_{72}Ge_{28}$ and temperature evolution is compared to those of bonded pairs in pure Au and $Au_{81}Si_{19}$ liquids. In Fig. 4, we report the most abundant bonded pairs, i.e. 142 *x* (sum of 1422 and 1421), 1431 and 15 *xx* pairs found in the three systems. The number of 15 *xx* bonded pairs is a direct measure of the degree of icosahedral ordering including both perfect and distorted icosahedral motifs, while 142 *x* bonded pairs are characteristic of close-packed structures (fcc and hcp). The 1431 pairs either can be considered as distorted icosahedra or distorted close-packed structures.[6] As they are similar in the three systems and hold steady with temperature, they are not considered responsible for differences between systems and/or as a function of temperature. In comparison with pure liquid Au, the fraction of 15 *xx* found in $Au_{72}Ge_{28}$ decreases with the Ge alloy, but the alloying effect is less

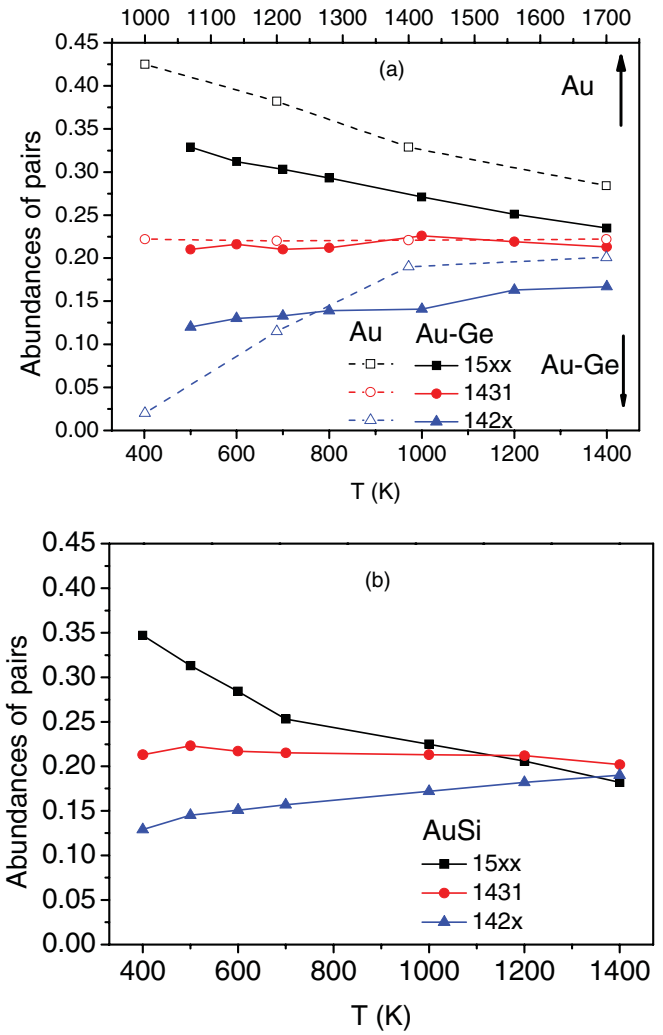

FIG. 4. (Color online) Evolution of abundances of pairs for Au, (a) $Au_{72}Ge_{28}$, and (b) $Au_{81}Si_{19}$ as a function of temperature. See text for more details.

important than that observed for $Au_{81}Si_{19}$ (Fig. 4). It means that the fraction of the icosahedral symmetry found in the liquid phase is more important in $Au_{72}Ge_{28}$ than in $Au_{81}Si_{19}$. In contrast also with the results obtained for $Au_{81}Si_{19}$, which displays a huge evolution of the icosahedral symmetry in the undercooled regime, the undercooled effect on the icosahedral symmetry in $Au_{72}Ge_{28}$ is much less important, similar to that of pure Au. At the same time, the evolution of 142 *x* pairs in both alloys is quite similar. The interesting result is that the fraction of 15 *xx* in the liquid phase after the Ge alloying is more important than that observed after the Si alloying. This difference can be related to the different CSROs obtained in the two liquids since alloying effects in such eutectic systems lead to a decrease of the icosahedral symmetry.[9] Less important is CSRO, and more important is ISRO. Such a situation is quite opposite to what is observed in binary Cu-Zr alloys that can be vitrified in bulk metallic glasses, since alloying effects in these alloys lead to an enhancement of the icosahedral local symmetry.[24] We can conclude that the two alloys present two distinct local structures. Such a result is in agreement with recent first-principles electronic calculations that predict the existence of crystalline compounds around the eutectic compositions of both systems[13,14] but with different crystallographic structures. It may also explain why Au-Ge does not form the same kind of amorphous phase on rapid quenching of the liquid phase Au-Si.[25,26] Another important experimental difference concerns surface properties of liquid $Au_{81}Si_{19}$ and $Au_{72}Ge_{28}$. Indeed, the surface structure of the liquid $Au_{72}Ge_{28}$ eutectic does not exhibit the same extraordinary properties that we found for liquid eutectic $Au_{81}Si_{19}$, i.e. a strong layering normal to the surface that is accompanied by an in-plane 2D crystalline long-range order.[10] As discussed by Pershan *et al.*,[11] the strong difference in CSRO in the bulk phase can explain the difference between the surface properties of the two liquids.

B. Dynamic properties:

To identify the effects of the local structure on the dynamic properties of stable and undercooled $Au_{72}Ge_{28}$, we have monitored dynamic properties of $Au_{72}Ge_{28}$ by first evaluating the mean-square displacement (MSD) to determine the self-diffusion coefficients, *D*, as well as their evolution as a function of temperature shown in Fig. 5. In order to get the equilibrium solid phase, atoms have to diffuse over rather large distances, while the formation of metastable phases should be limited by diffusion processes in both liquid and solid phases. Therefore, diffusion processes are also important factors to explain the occurrence of stable or metastable solid phases at the eutectic composition. In the liquid state, the ballistic regime in the MSD is directly followed by a diffusive regime at long times from which *D* is extracted. At lower temperatures corresponding to the undercooled region, a well-known caging effect[27] takes place after the ballistic motion, delays the diffusive regime, and gives rise to the non-Arrhenius dramatic slowdown of *D*. We plot the values of *D* in Fig. 5 and compare them to those of pure Au and $Au_{81}Si_{19}$. To our knowledge, there is no experimental data for $Au_{72}Ge_{28}$, but we report those obtained for pure Au and $Au_{81}Si_{19}$. For $Au_{81}Si_{19}$, the values of *D* are in

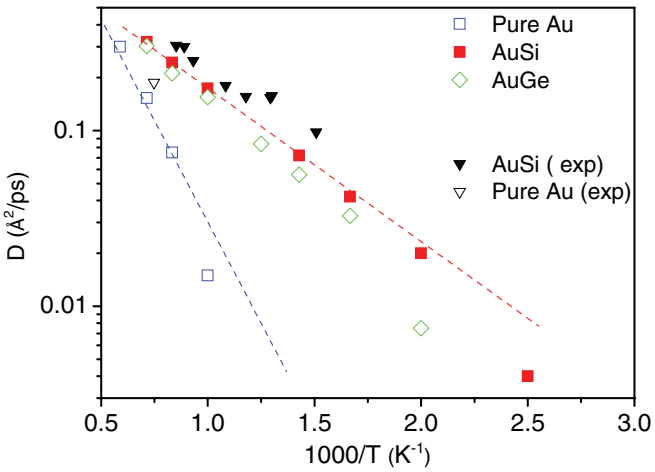

FIG. 5. (Color online) Evolution of the self-diffusion coefficients for Au (open squares), $Au_{72}Ge_{28}$ (diamond), and $Au_{81}Si_{19}$ (full squares) as a function of temperature. The open triangle corresponds to the experimental value of liquid Au at the melting point inferred from the viscosity data of Ref. 29, and the full triangles are the experimental data of Ref. 28 of $Au_{81}Si_{19}$ in the liquid state.

good agreement with the experimental data[28] in the liquid state and display the same evolution with temperature. For pure Au at the melting point, the value of D is close to that inferred from the viscosity measurements[29] by using the Stokes–Einstein relation. Note that the self-diffusion coefficients of Au and Ge species in the alloy are very similar as in Au-Si, and then the self-diffusion coefficient of the alloy gives direct information about the Ge-alloying effect on the diffusivity of Au atoms.

At the temperature corresponding to the melting of pure Au, the diffusivity of the $Au_{72}Ge_{28}$ liquid is found to be twice that of pure liquid Au and similar to that of $Au_{81}Si_{19}$. At the eutectic temperature, $Au_{72}Ge_{28}$ still displays a diffusivity characteristic of a liquid phase, but less pronounced than $Au_{81}Si_{19}$. Such a difference can be related to a more pronounced ISRO in $Au_{72}Ge_{28}$. As discussed in Ref. 9 for $Au_{81}Si_{19}$, the diffusivity by the Ge-alloying effect can be related to dynamical correlations. Because of their high density, the back-scattering regime is predominant for pure Au, $Au_{72}Ge_{28}$, and $Au_{81}Si_{19}$ liquids. As the backscattering effect is directly related to the occurrence of icosahedral motifs in the liquid phase,[9] it is very pronounced in pure Au and more in $Au_{72}Ge_{28}$ than in $Au_{81}Si_{19}$ and explains the sequence obtained for the values of the self-diffusion coefficients of the three systems.

We come now to the discussion of the evolution of diffusivity as a function of temperature, as shown in Fig. 5. While it is Arrhenius for $Au_{72}Ge_{28}$ in the liquid state, it becomes non-Arrhenius below the eutectic point with a more rapid decrease of D. Such an evolution also holds for $Au_{81}Si_{19}$ but at a lower temperature. As mentioned above, below the eutectic points, the increase of the 15 xx-bonded pairs is seen in both systems but with different slopes. It is worth mentioning that such an increase of the icosahedral ordering associated to a non-Arrhenius evolution of the diffusivity is a characteristic feature of fragile liquids.[30,31] Clearly, the development of an icosahedral ordering in the undercooled regime leads to a more pronounced backscattering effect and then is directly responsible for the slowdown of the dynamics in the undercooled liquid.[9] As the ISRO is more important in $Au_{72}Ge_{28}$, it explains why the non-Arrhenius behavior occurs at higher temperature than in $Au_{81}Si_{19}$.

This is confirmed from the temperature evolution of the relaxation time scale characteristic of the system, which is related to the α relaxation time τ_α. The latter can be determined through the self-intermediate scattering function describing the relaxation dynamics.[32] Figure 6 compares the results of τ_α for Au-Ge with those of Au-Si. As expected, the α relaxation visibly increases in a non-Arrhenius manner for both systems. However, the dynamical slowdown is more pronounced for Au-Ge than for Au-Si due to the higher degree of ISRO. As the α relaxation time is related to the viscosity,[32] Au-Ge eutectic liquid has a higher viscosity when it is cooled toward the glass transition temperature and therefore has lower fragility[30] than Au-Si, which is consistent with the difference in the evolution of their ISRO in the undercooled region. This has consequences on the formation of their amorphous states and can explain why they are different.[25,26]

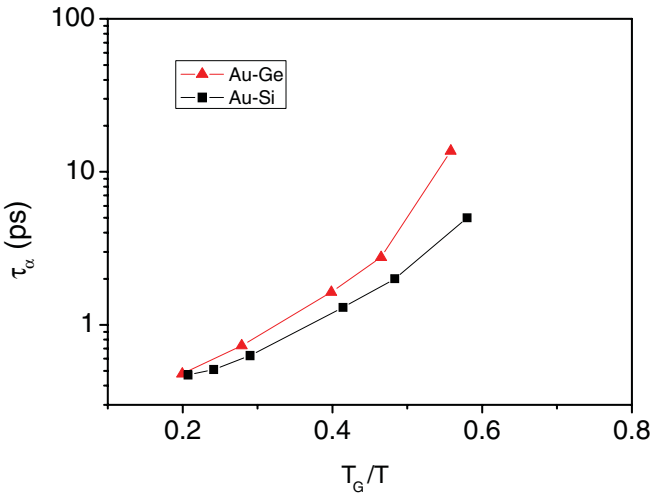

FIG. 6. (Color online) Evolution of the α relaxation time for $Au_{72}Ge_{28}$ (red triangles) and $Au_{81}Si_{19}$ (black squares) as a function of inverse temperature scaled by the experimental glass transition temperature T_G, which are respectively 279 and 291 K (Ref. 33).

IV. CONCLUSION

In summary, the results presented here enable us to show that the Ge-alloying effect on the local structure of the eutectic liquid $Au_{72}Ge_{28}$ alloy is quite different to that observed in the eutectic $Au_{81}Si_{19}$ liquid alloy. On one side, the local structure of the eutectic $Au_{72}Ge_{28}$ alloy shows a weak CSRO and only in the undercooled regime, in contrast to the very high CSRO observed in the stable and uncerdooled $Au_{81}Si_{19}$ liquids. On the other side, the weakness of Au-Ge bonds as compared to Au-Si ones leads to a more pronounced ISRO in $Au_{72}Ge_{28}$ and a variation of ISRO in the undercooled regime that is closer to Au than to $Au_{81}Si_{19}$. The icosahedral increase that occurs below the eutectic temperature of two systems is responsible for the non-Arrhenius evolution of their diffusivity. Note that in $Au_{72}Ge_{28}$, the non-Arrhenius behavior occurs at higher temperature, and the fragility is lower due to more abundant icosahedral motifs in this eutectic alloy. We believe that such differences in the local structure can explain largely the observed differences in the bulk and surface properties of the two systems.

ACKNOWLEDGMENTS

We acknowledge the CINES (Centre Informatique National de l'Enseignement Supérieur) and IDRIS (Institut du Développement et des Ressources en Informatique) under Project No. INP2227/72914 as well as PHYNUM CIMENT (Calcul Intensif / Modélisation / Expérimentation Numérique et Technologique) for computational resources.

*noel.jakse@grenoble-inp.fr

[1] D. Turnbull, J. Chem Phys. **20**, 11 (1951).
[2] F. C. Frank, Proc. R. Soc. London A **215**, 1022 (1950).
[3] H. W. Sheng, W. K. Luo, F. M. Alamgir, J. M. Bai, and E. Ma, Nature **439**, 419 (2006).
[4] T. Schenk, D. Holland-Moritz, V. Simonet, R. Bellissent, and D. M. Herlach, Phys. Rev. Lett. **89**, 075507 (2002).

[5]G. W. Lee, A. K. Gangopadhyay, K. F. Kelton, R. W. Hyers, T. J. Rathz, J. R. Rogers, and D. S. Robinson, Phys. Rev. Lett. **93**, 037802 (2004).
[6]N. Jakse and A. Pasturel, Phys. Rev. Lett. **91**, 195501 (2003); N. Jakse, O. LeBacq, and A. Pasturel, Phys. Rev. B **70**, 174203 (2004); N. Jakse and A. Pasturel, J. Chem. Phys. **120**, 6124 (2004); Mod. Phys. Lett. B **20**, 655 (2006); Phase Transitions **80**, 369 (2007).
[7]T. B. Massalski, *Binary Alloy Phase Diagrams*, 2nd ed. (American Society for Metals International, Materials Park, Ohio, 1990), p. 428.
[8]T. U. Schülli, R. Daudin, G. Renaud, A. Vaysset, O. Geaymond, and A. Pasturel, Nature (London) **464**, 1137 (2010).
[9]A. Pasturel, E. S. Tasci, M. H. F. Sluiter, and N. Jakse, Phys. Rev. B **81**, 140202(R) (2010).
[10]O. G. Shpyrko, R. Streitel, V. S. K. Balagurusamy, A. Y. Grigoriev, M. Deutsch, B. M. Ocko, M. Meron, B. Lin, and P. S. Pershan, Phys. Rev.B **76**, 245436 (2007).
[11]P. S. Pershan, S. E. Stoltz, S. Mechler, O. G. Shpyrko, A. Y. Grigoriev, V. S. K. Balagurusamy, B. H. Lin, and M. Meron, Phys. Rev. B **80**, 125414 (2009).
[12]S. Takeda, H. Fujii, Y. Kawakita, S. Tahara, S. Nakashima, S. Kohara, and M. Itou, J. Alloys Compd. **452**, 149 (2008).
[13]E. S. Tasci, M. H. F. Sluiter, A. Pasturel, and P. Villars, Acta Mater. **58**, 449 (2010).
[14]E. S. Tasci, M. H. F. Sluiter, A. Pasturel, and N. Jakse, Phys. Rev. B **81**, 172202 (2010).
[15]G. Kresse and J. Furthmüller, Comput. Mater. Sci. **6**, 15 (1996).
[16]G. Kresse and D. Joubert, Phys. Rev. B **59**, 1758 (1999).
[17]P. Chirawatkul, A. Zeidler, P. S. Salmon, S. Takeda, Y. Kawakita, T. Usuki, and H. E. Fischer, Phys. Rev. B **83**, 014203 (2011).
[18]F. H. Stillinger and T. A. Weber, Phys. Rev. A **25**, 978 (1982).
[19]W. Hoyer and R. Jödicke, J. Non-Cryst. Solids **192–193**, 102 (1995).
[20]R. M. Waghorne, V. G. Rivlin, and G. I. Williams, J. Phys. F: Metal Phys. **6**, 147 (1976).
[21]C. N. J. Wagner and H. Ruppersberg, At. Energy Rev. **1**, 101 (1981).
[22]H. S. Chen and D. Turnbull, J. Appl. Phys. **38**, 3646 (1967).
[23]J. D. Honeycutt and H. C. Andersen, J. Phys. Chem. **91**, 4950 (1987).
[24]N. Jakse and A. Pasturel, Appl. Phys. Lett. **93**, 113104 (2008); Phys. Rev. B **78**, 214204 (2008).
[25]P. Ramachandrarao and T. R. Anantharaman, Trans. Metall. Soc. AIME **245**, 886 (1969).
[26]W. Klement, R. H. Willens, and P. Duwez, Nature (London) **187**, 869 (1960).
[27]W. Kob, J. Phys. Condens. Matter **11**, R85 (1999).
[28]A. Bruson and M. Gerl, J. Appl. Phys. **53**, 3616 (1982).
[29]T. Iida and I. L. Guthrie, *The Physical Properties of liquid Metals* (Clarendon, Oxford, 1988), p. 158.
[30]C. A. Angell, Science **267**, 1924 (1995).
[31]H. Tanaka, J. Phys.: Condens. Matter **15**, L491 (2003).
[32]K. Binder and W. Kob, *Glassy Materials and Disordered Solids*, (World Scientific Publishing, Singapore, 2005).
[33]H. S. Chen and D. Turnbull, J. Chem. Phys. **48**, 2560 (1968).